ISSN 1070-3632, Russian Journal of General Chemistry, 2013, Vol. 83, No. 12, pp. 2395–2401. © Pleiades Publishing, Ltd., 2013.

Synthesis, Experimental, and DFT Studies on FT–IR, ^{1}H, and ^{13}C NMR Spectra of Azo-Linked Dihydropyridines[1]

L. Zare Fekri[a] and M. Nikpassand[b]

[a] *Department of Chemistry, Payame Noor University, PO Box 19395-3697 Tehran, Iran*
email: chem_zare@pnu.ac.ir; chem_zare@yahoo.com

[b] *Department of Chemistry, Rasht Branch, Islamic Azad University, Rasht, Iran*

Received August 8, 2013

Abstract—An efficient one-pot synthesis of dihydropyridines by solid state three-component condensation reactions of aldehydes, dimedone, and ammonium acetate in the presence of HY-Zeolite has been achieved. The conversion took short time to form the products in excellent yields. HY-Zeolite can be recovered and reused. Density Functional Theory (DFT) calculations at the B3LYP level is used to optimize the geometry and calculate FT–IR, ^{1}H, and ^{13}C NMR spectra of the compounds. We found that the calculated values are in accordance with the experimental data.

DOI: 10.1134/S1070363213120347

INTRODUCTION

1,4-Dihydropyridine is a common feature of various biological compounds such as antibacterial, anti-inflammatory, calcium antagonist and anti tyrosine kinase inhibiting agents [1–4].

The classical method for the synthesis of dihydropyridines involves the three-component condensation of an aldehyde with ethyl acetoacetate and ammonia in acetic acid or refluxing alcohol [5]. However, these methods suffer from drawbacks like long reaction time, use of an excess of organic solvent, and low yields of the products. Yet a number of modified methods under improved conditions by using microwave irradiation [6], ionic liquids [7], molecular iodine [8], cerium ammonium nitrate [9], polymers [10], and organo-catalyst [11] was developed. However, the use of high temperatures, expensive metal precursors, catalysts that are harmful to environment, unsatisfactory yields and long reaction time limit the use of these methods. Moreover, the main disadvantage of almost all existing methods is that the catalysts are destroyed in the work-up procedure and cannot be recovered or reused. Therefore, the search continues for the synthesis of dihydropyridines in terms of operational simplicity, reusability, economic viability, and greater selectivity.

[1] The text was submitted by the authors in English.

EXPERIMENTAL

Materials and measurements. Chemicals were purchased from Merck and Fluka and used as purchased. Melting points were measured on an Electro-thermal 9100 apparatus and were uncorrected. ^{1}H NMR spectra were obtained on a Bruker DRX 500 in DMSO as solvent and with TMS as internal reference. FT–IR spectra were recorded on a Shimadzu FT–IR-8400S spectrometer. Elemental analyses were carried out on a Carlo-Erba EA1110CNNO-S analyzer.

In recent years, HY-Zeolite has received considerable attention as a mild Lewis acid for a number of organic transformations because the catalyst is green and reusable. As a part of the continuing effort in our laboratory toward the development of new methods in organic synthesis for the synthesis of heterocyclic and pharmaceutical compounds, [12–14] we became interested in the possibility of developing a one-pot synthesis of dihydropyridines derivatives through the Hantzsch reaction of aldehydes, dimedone, and ammonium acetate in the presence of a reusable HY-Zeolite catalyst under solid state condition (Scheme 1).

We have examined other Lewis acids such as KSF, bentonite, MCM-41, and K10 for this reaction (Table 1), and HY-Zeolite was found to be the most effective catalyst in terms of conversion and reaction rates. To

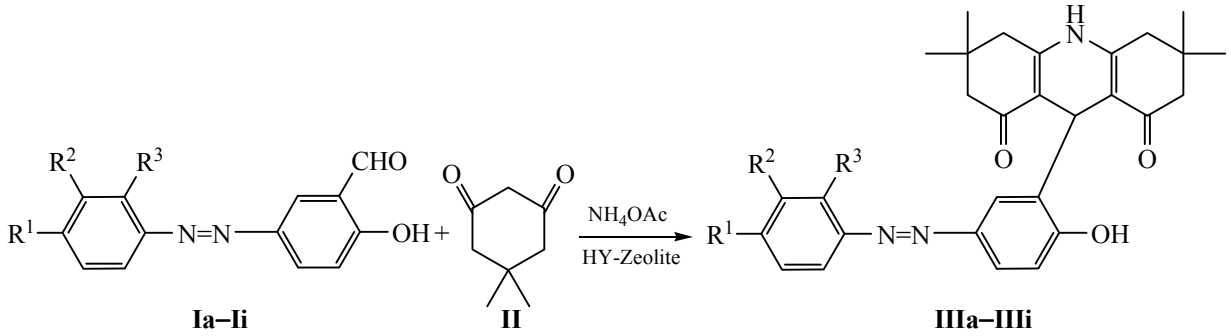

Ia–Ii **II** **IIIa–IIIi**

Scheme 1. Synthetic route to azo-linked dihydropyridines.

achieve suitable conditions for the synthesis of fused heterocyclic dihydropyridines, we investigated the reaction of azo-linked benzaldehyde **I**, dimedone **II**, and ammonium acetate in the presence of HY-Zeolite in different conditions. In refluxing alcohol the reaction was very slow and the yield of product was very low. We found that the best results were obtained in the presence of HY-Zeolite under solid state conditions.

Apart from the mild conditions of the process and its excellent results, the simplicity of product isolation, replacement of carcinogenic solvent with solvent-free process and the possibility to recycle HY-zeolite offer a significant advantage.

General procedure for the synthesis of Va–Vi in the presence of HY-Zeolite under solid state condition. A mixture of aldehyde (1 mmol), dimedone (2 mmol), NH_4OAc (1 mmol), and HY-Zeolite (0.1 g) without solvent was heated at 60°C for the required reaction time (Table 1). When the reaction was stopped, the mixture was washed with $CHCl_3$ to separate the organic compound and HY-Zeolite. The organic compound was purified by column chromatography to produce 1,4-dihydropyridine derivatives **IIIa–IIIi** as pure crystalline products.

Computational details. The geometries were optimized at the B3LYP level of theory along with standard 6-31G(d) basis set as shown in Fig. 1. The harmonic vibrational frequencies and their relative intensities were calculated by this method and the results were compared with experimental FT–IR spectrum. The most widely used technique for calculating NMR shielding tensors is the GIAO (Gauge Including Atomic Orbital) method. This method was used for calculating ^1H and ^{13}C NMR chemical shifts at the B3LYP/6-31G(d) level. All the calculations were carried out with the Gaussian03 software.

The structure and the scheme of atoms numbering in **IIIa, IIIc**, and **IIId** are shown in Fig. 2.

The observed and calculated frequencies using DFT B3LYP/6-31G and their probable assignments for **IIIa,**

Table 1. Synthesis of azo-linked dihydropyridines under solid state condition

Run no.	R^1	R^2	R^3	Product	Time, min	Yield, %[a,b]	mp, °C (observed)	mp, °C (publ.)
1	H	H	H	**IIIa**	8	82	180–182	186–188
2	Me	H	H	**IIIb**	10	85	159–160	160–162
3	Et	H	H	**IIIc**	10	81	130–132	129–131
4	NO_2	H	H	**IIId**	5	95	250–251	248–250
5	Cl	H	H	**IIIe**	5	94	166–167	165–167
6	H	Cl	H	**IIIf**	5	85	267–268	265–267
7	Br	H	H	**IIIg**	3	87	170–171	171–173
8	H	H	Cl	**IIIh**	5	84	166–167	167–169
9	I	H	H	**IIIi**	4	87	145–147	148–150

[a] Isolated yields. [b] All products were characterized by comparison of their mp, IR, and NMR spectra with those of authentic samples [11].

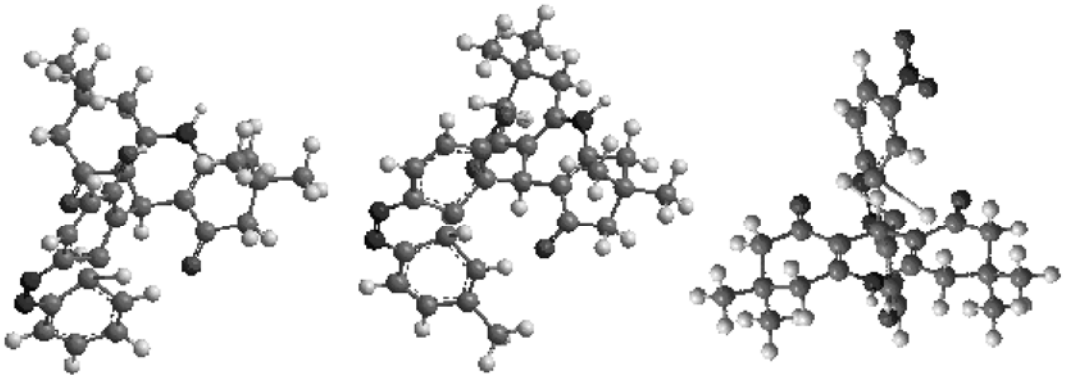

IIIa X = H **IIIb** X = CH_3 **IIId** X = NO_2

Fig. 1. The geometry optimization of the selected synthesized compounds.

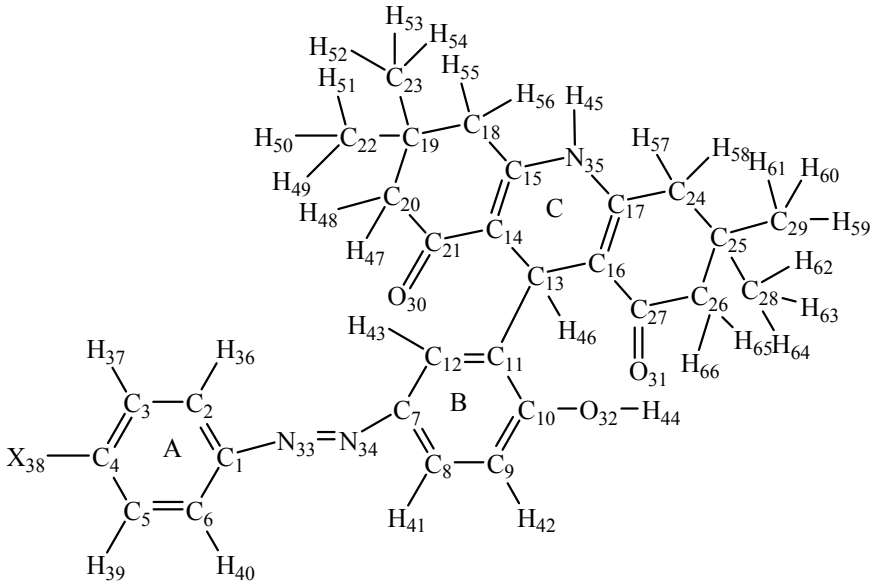

Fig. 2. Structure, atom, and ring numbering scheme of **IIIa, IIIb,** and **IIId.**

IIIb, and **IIId** are summarized in Table 3. The C=C stretching vibration bands appeared in the infrared spectrum at 1600–1425 cm^{-1}. The bands occurring at 1375 in **IIIa**, 1313 in **IIIb**, and 1340 in **IIId** in the IR spectra are assigned to the ring C–N stretching vibrations. The C=O stretching vibration bands are calculated at 1645 in **IIIa**, 1654 in **IIIb**, and 1645 in **IIId**. The bands observed in the infrared spectra of **IIIa** at 3342, 3394 in **IIIb**, and 3272 in **IIId** are assigned to the N–H stretching vibrations. The asymmetric and symmetric stretching vibrations of the nitro group are the most intense bands of the spectrum. The frequencies observed at 1519 cm^{-1} in the infrared spectrum are assigned to the $–NO_2$ asymmetric stretching modes of **IIId**. The very strong symmetric stretching vibration of nitro group of the compound is assigned to the wave number 1371 cm^{-1} in the infrared spectrum. The correction factors used to correlate the experimentally observed and theoretically computed frequencies for each vibrational mode of **IIIa, IIIb,** and **IIId** under DFT-B3LYP method are similar. The linear regression between the experimental and theoretical wave number of **IIIa, IIIb,** and **IIId** is shown in Fig. 3. Thus, vibrational frequencies calculated by using the B3LYP functional with 6-31G basis sets can be utilized to eliminate the uncertainties in the fundamental assignments in infrared vibrational spectra.

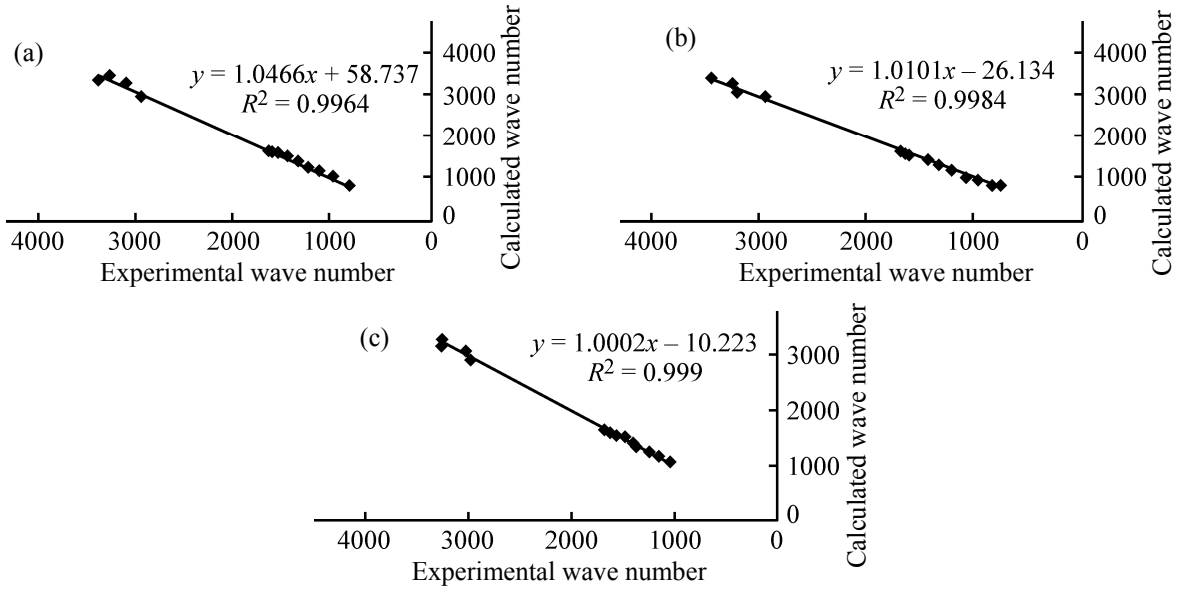

Fig. 3. Correlation plot of experimental and theoretical IR of (a) **IIIa,** (b) **IIIb,** and (c) **IIId** at the B3LYP/6-31G(d) level.

The ^{1}H and ^{13}C theoretical and experimental chemical shifts, isotropic shielding tensors and the assignments ofsignals in the spectra of **IIIa, IIIb,** and **IIId** are presented in Table 4 and Table 5, respectively. Aromatic carbons give signals in overlapped areas of the spectrum with chemical shift values from 100 to 150 ppm in ^{13}C NMR and 6–8.5 ppm in ^{1}H NMR spectra of **IIIa, IIIb,** and **IIId**.

Table 2. The observed FT–IR and frequencies calculated using B3LYP/6-31G(d) force field

Assignment	IIIa		IIIb		IIIc	
	calculated	experimental	calculated	experimental	calculated	experimental
ν(N–H)	3365.2147	3342	3412.1010	3394	3257.1465	3272
ν(O–H)	3254.3697	3456	3214.5891	3250	3250.1023	3197
ν(C–H) aromatic	3079.3158	3255	3175.3584	3103	3017.8657	3064
ν(C–H) aliphatic	2936.8913	2952	2910.3248	2999	2965.6522	2927
ν(C=O)	1645.3821	1641	1654.2559	1649	1645.2154	1612
ν(NO_2)	–	–	–	–	1385.6578	1371
ν(NO_2)	–	–	–	–	1555.3248	1519
ν(N=N)	1465.2139	1481	1445.3695	1431	1475.2189	1481
ν(C=C)	1601.9812	1591	1610.6875	1600	1610.9521	1600
ν(C=C)	1543.8745	1558	1414.3225	1425	1465.2147	1479
ν(C–O)	1254.3125	1249	1220.3212	1228	1229.3165	1228
ν(C–N)	1359.6544	1375	1330.2549	1313	1359.7831	1340
β(HCC)	1140.3654	1151	1076.3651	1020	1024.7898	1014
β(HCC)	1006.2126	1020	1042.5954	1000	1141.6524	1141
β(HCC)	1240.3555	1220	963.2544	962	1175.4562	1150
γ(C–H)	850.5454	829	836.3214	823	875.4352	852

Table 3. The experimental and calculated ^{1}H isotropic chemical shifts (ppm) with respect to TMS of **IIIa–IIIc**

Assignment	IIIa		IIIb		IIIc	
	calculated	experimental	calculated	experimental	calculated	experimental
H_{51},H_{50},H_{49}	1.07	1.04	0.6	0.94	0.59	0.89
H_{52}, H_{53},H_{54}	1.34	1.14	0.5	0.84	0.6	1.00
H_{61}, H_{60},H_{59}	1.03	1.04	0.43	0.84	0.44	0.89
H_{62}, H_{63},H_{64}	1.34	1.14	0.58	0.94	0.52	1.00
H_{47},H_{48}	2.34	2.29	1.68	2.50	1.79	2.50
H_{55}, H_{56}	1.81	1.92	1.51	2.07	1.54	2.10
H_{58}, H_{57}	1.99	2.05	1.46	1.93	1.45	1.99
H_{65}, H_{66}	2.27	2.12	1.56	2.35	1.58	2.15
H_{46}	4.62	4.70	3.88	5.1	3.73	4.8
H_{36}	7.65	7.15	7.91	7.68	7.93	7.90
H_{40}	6.06	7.15	7.84	7.68	7.14	7.90
H_{37}	7.56	7.47	7.18	7.32	6.68	8.35
X_{38}	6.51	7.44	1.21	2.23	–	–
H_{39}	6.59	7.47	6.85	7.32	8.7	8.35
H_{41}	7.12	7.77	7.79	7.6	6.84	7.64
H_{42}	7.85	7.83	6.55	7.09	6.65	6.87
H_{43}	7.01	7.62	7.34	7.46	7.84	7.62

The downfield chemical shift of C_{15} rather than C_{14} is observed in **IIIa, IIIb**, and **IIId**. That is due to the mesomeric effect between C^{15}–C^{14}–C^{21}–O^{30}. The benzylic and allylic C–H carbon atom (C^{13}) is calculated at 26.7 in **IIIa**, 27.24 in **IIIb**, and 31.2 in **IIId** in relatively good accordance with experimental results. Similarly, the benzylic and allylic C–H proton atom (H^{46}) appeared at 4.7 in **IIIa**, 5.1 in **IIIb**, and 4.8 in **IIId** in according to their resonated chemical shift in the experimental results. The calculated and experimental chemical shift values given in Tables 4 and 5 show a good agreement with each other. The linear regression between the experimental and theoretical ^{1}H and ^{13}C NMR chemical shifts of **IIIa, IIIb**, and **IIId** are presented in Figs. 4–6.

CONCLUSIONS

Consequently, we have developed an efficient, green, fast, and convenient procedure for the synthesis of 1,4-dihydropyridines through the three component

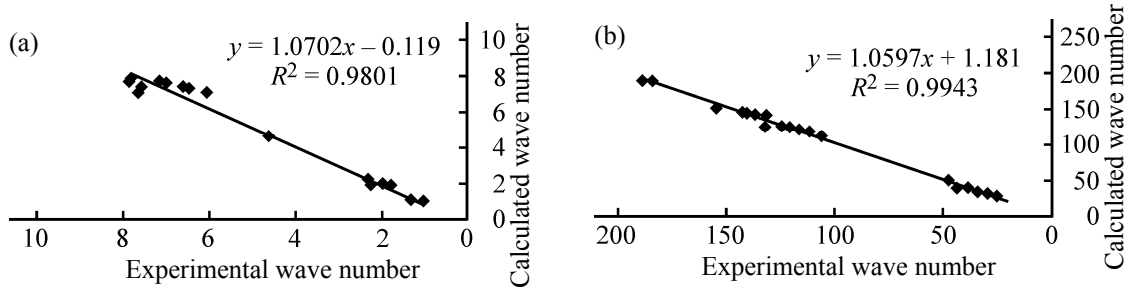

Fig. 4. Correlation plots of experimental and theoretical (a) ^{1}H and (b) ^{13}C NMR chemical shifts of **IIIa** at the B3LYP/6-31G(d) level.

condensation of aldehydes, dimedone and ammonium acetate over K10 Zeolite under solid state conditions. The geometries of **IIIa, IIIb**, and **IIId** were optimized with DFT-B3LYP using 6-31G basis sets. The vibration frequencies of the fundamental modes of the compound have been precisely assigned and analyzed and the theoretical results were compared with the experimental vibrations. ^{1}H and ^{13}C NMR isotropic chemical shifts were calculated and the assignments made were compared with the experimental values.

Table 4. The experimental and calculated ^{13}C isotropic chemical shifts (ppm) with respect to TMS of **IIIa–IIIc**

Assignment	**IIIa**		**IIIb**		**IIIc**	
	calculated	experimental	calculated	experimental	calculated	experimental
C_4	111.05	121.6	120.48	128.7	149.7	135.88
C_3	131.29	130.0	127.73	140.7	133.4	117.29
C_5	123.85	130.0	126.99	140.7	146.8	135.93
C_2	115.46	126.2	114.39	124.0	123.8	121.26
C_6	116.86	126.2	119.02	124.0	121.2	125.71
C_1	153.5	157.3	150.92	160.2	157.9	146.25
C_7	141.52	150.8	143.61	156.2	144.86	144.86
C_8	122.73	129.5	122.97	131.2	129.9	122.21
C_9	119.55	127.0	119.84	125.5	129.8	122.01
C_{10}	139.54	149.3	142.36	153.3	152.9	141.44
C_{11}	112.42	123.5	112.96	121.2	123.8	114.03
C_{12}	105.19	111.5	115.72	113.5	114.9	120.23
C_{13}	26.7	27.9	27.24	31.1	31.2	27.73
C_{14}	105.3	119.2	105.26	118.2	123.5	105.14
C_{21}	182.45	196.3	180.93	198.2	198.8	181.62
C_{20}	47.56	51.7	45.37	52.5	42.7	44.85
C_{19}	28.86	30.0	30.39	32.3	50.2	29.9
C_{18}	43.95	40.1	37.45	41.8	33.6	37.19
C_{15}	135.83	147.6	133.75	146.4	132.0	134.12
C_{22}	25.66	34.4	26.95	26.6	28.0	26.92
C_{23}	33.21	34.4	20.46	26.6	28.0	20.3
C_{16}	106.23	119.2	105.75	118.2	123.5	105.32
C_{27}	186.92	196.3	180.38	198.2	198.8	181.21
C_{26}	48.17	51.7	44.74	52.5	42.7	44.69
C_{25}	24.45	30.0	29.54	32.3	50.2	29.73
C_{24}	38.86	40.1	37.04	41.8	33.6	36.9
C_{17}	130.58	147.6	132.88	146.4	132.0	134.1
C_{29}	33.76	34.4	26.89	23.0	28.0	20.26
C_{28}	30.13	34.4	20.25	23.0	28.0	26.81

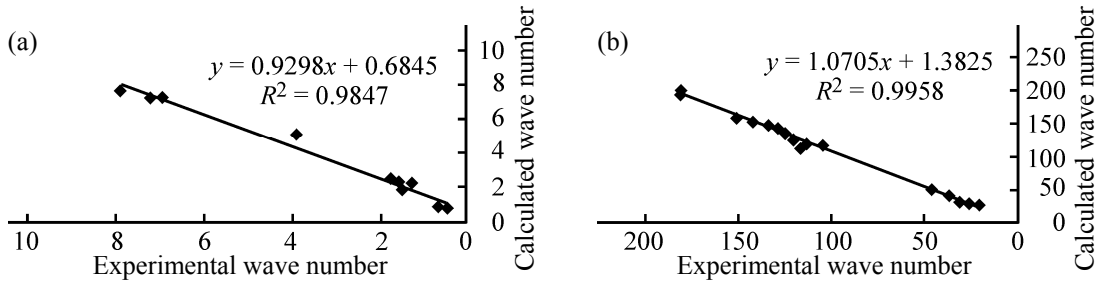

Fig. 5. Correlation plots of experimental and theoretical (a) ^{1}H and (b) ^{13}C NMR chemical shifts of **IIIb** at the B3LYP/6-31G(d) level.

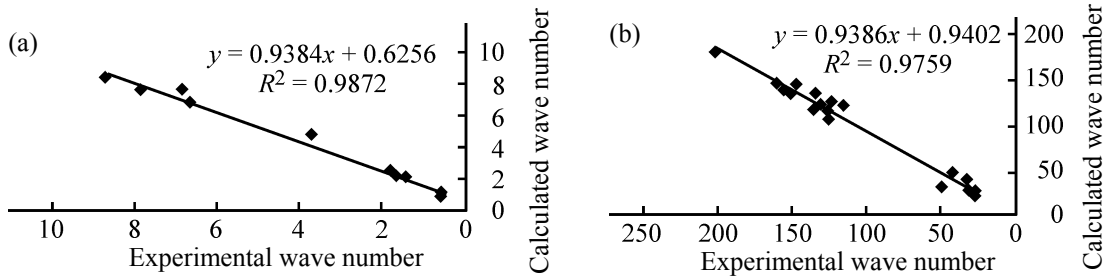

Fig. 6. Correlation plots of experimental and theoretical (a) ^{1}H and (b) ^{13}C NMR chemical shifts of **IIId** at the B3LYP/6-31G(d) level.

Thus the present investigation provides complete vibration assignments, structural information, and chemical shifts of the compounds under study.

ACKNOWLEDGMENTS

We thank the Research Committee of Islamic Azad University of Rasht Branch for partial support given to this study.

REFERENCES

1. Godfraid, T., Miller, R., and Wibo, M., *Pharmacol. Rev*., 1986, vol. 38, pp. 321–416.
2. Chen, Y.L., Fang, K.C., Sheu, J.Y., Hsu, S.L., and Tzeng, C.C., *J. Med. Chem*., 2001, vol. 44, pp. 2374–2377.
3. Roma, G., Braccio, M.D., Grossi, G., and Chio, M., *Eur. J. Med. Chem*., 2000, vol. 35, pp. 1021–1035.
4. Maguire, M.P., Sheets, K.R., Mcvety, K., Spada, A.P., and Zilberstein, A., *J. Med. Chem*., 1994, vol. 37, pp. 2129–2137.
5. Margarita, S., Yamila, V., Estael, M., Nazario, M., Roberto, M., Margaria, Q., Carlos, S., Jose, S., Hector, L.N., Norbert, B., Oswald, M., and Camiel, D., *J. Heterocycl. Chem*., 2000, vol. 37, pp. 735–742.
6. Agarwal, A. and Chauhan, P.M.S., *Tetrahedron Lett*., 2005, vol. 46, pp. 1345–1348;
7. Ji, S.J., Jiang, Z.Q., Lu, J., and Loh, T.P., *Synlett,* 2004, pp. 831–835.
8. Ko, S., Sastry, M.N.V., Lin, C., and Yao, C.F., *Tetrahedron Lett*., 2005, vol. 46, pp. 5771–5774.
9. Ko, S. and Yao, C.F., *Tetrahedron,* 2006, vol. 62, pp. 7293–7299.
10. Dondoni, A., Massi, A., Minghini, E., and Bertolasi, V., *Tetrahedron*, 2004, vol. 60, pp. 2311–2326.
11. Kumar, A. and Maurya, R.A., *Tetrahedron*, 2007, vol**.** 63, pp.1946–1952.
12. Nikpassand, M., Mamaghani, M., Tabatabaeian, K., and Kupaei Abiazi, M., *Molecular Diversity*, 2009, p. 389.
13. Nikpassand, M., Mamaghani, M., and Tabatabaeian, K., *Molecules,* 2009, vol. 14, pp. 1468–1476.
14. Nikpassand, M., Zare, L., and Saberi, M., *Monat. fur Chemie*, 2012, pp. 143, pp. 289–293.